

Potent and Highly Selective Inhibitors of the Protein Tyrosine Phosphatase 1B[†]

Meng Taing,^{‡,||} Yen-Fang Keng,^{§,||} Kui Shen,^{‡,||} Li Wu,[§] David S. Lawrence,^{*,‡} and Zhong-Yin Zhang^{*,‡,§}

Departments of Biochemistry and Molecular Pharmacology, The Albert Einstein College of Medicine of Yeshiva University, 1300 Morris Park Avenue, Bronx, New York 10461

Received June 10, 1998; Revised Manuscript Received November 16, 1998

ABSTRACT: Several protein tyrosine phosphatases (PTPases) have been implicated as regulatory agents in the insulin-stimulated signal transduction pathway, including PTP1B, PTP α , and LAR. Furthermore, since all three enzymes are suggested to serve as negative regulators of insulin signaling, one or more may play a pivotal role in the pathogenesis of insulin resistance. We report herein the acquisition of highly selective PTP1B-targeted inhibitors. We recently demonstrated that PTP1B contains two proximal aromatic phosphate binding sites [Puius, Y. A., Zhao, Y., Sullivan, M., Lawrence, D. S., Almo S. C., and Zhang, Z. Y. (1997) *Proc. Natl. Acad. Sci. U.S.A.* 94, 13420–5], and we have now employed this structural feature to design and synthesize an array of bis(aryldifluorophosphonates). Not only do the lead compounds serve as potent inhibitors of PTP1B but, in addition, several exhibit selectivities for PTP1B versus PTP α , LAR, and VHR that are greater than 2 orders in magnitude.

Signal transduction pathways serve as a highly efficient mechanism by which events that transpire at the cell surface are conveyed as biochemical signals to remote subcellular sites. These phosphoryl-transfer-driven pathways confer upon the cell an ability to respond, both rapidly and reversibly, to external stimuli. Although the role of individual protein kinases in many of these pathways still awaits complete resolution, the basic framework of several pathways has now been elucidated. Furthermore, defects in protein kinase activity have been linked to a variety of disease states. Consequently, in those instances where protein kinase action is inappropriately high, protein kinase inhibitors may constitute a valuable new family of therapeutic agents (1). Protein kinases catalyze the formation of serine, threonine, and tyrosine phosphomonoesters, species that can be readily hydrolyzed by protein phosphatases to the corresponding starting alcohols. It is the relatively metastable nature of the phosphomonoester moiety that confers the desirable trait of rapid signal termination exhibited by these pathways. Although protein phosphatases are integral components of signal transduction, until recently research on the structure and enzymology of protein phosphatases has lagged considerably behind that of the protein kinases (2). Indeed, the precise in vivo role of individual protein phosphatases still remains largely an enigma.

PTP1B was the first protein tyrosine phosphatase (PTPase) to be purified to homogeneity (3–4). The enzyme is widely expressed in insulin-sensitive tissues (5). Recent studies have demonstrated that PTP1B is a negative regulator of the insulin-stimulated signal transduction pathway. PTP1B an-

tibody-loaded cells exhibit an enhanced response to insulin stimulation (6). Cell lines overexpressing either wild type PTP1B or a catalytically inactive mutant likewise exhibit behavior consistent with the notion that PTP1B downregulates insulin-dependent signaling (7), likely via dephosphorylation of the insulin receptor. These results suggest that PTP1B inhibitors may be therapeutically beneficial in the treatment of Type II diabetes mellitus and insulin resistance. In addition to its role in insulin signaling, PTP1B is overexpressed in a large percentage of human breast cancer patients, implying that it plays an important role in cell proliferation (8). Indeed, recent studies have demonstrated that PTP1B associates with and dephosphorylates p130^{Cas}, a key component in mitogen-mediated signal transduction (9). In addition, Liu and Chernoff (10) have shown that PTP1B binds to and serves as a substrate for the epidermal growth factor receptor. These results, taken together, not only establish a direct role for PTP1B in intracellular signal transduction but also suggest that this PTPase may be a participant in several pathways.

PTP1 (the rat structural homologue of human PTP1B) coordinates phosphotyrosine, as well as a plethora of other aromatic phosphates, within its active site region (11). However, recently a second (noncatalytic) aryl phosphate binding site in PTP1B has been discovered, one which lies adjacent to the active site (12). Since the second aryl phosphate binding site is less conserved than the catalytic site, this unexpected structural motif suggests that compounds containing two appropriately conjoined phosphotyrosine analogues could serve as potent and highly selective inhibitors of PTP1B. We describe herein several PTPase inhibitors that exhibit selectivities of up to 2 orders of magnitude in favor of PTP1B relative to other PTPases.

MATERIALS AND METHODS

General Procedures. All moisture-sensitive reactions were carried out in oven-dried glassware under a positive pressure of dry nitrogen. Anhydrous tetrahydrofuran (THF), methylene chloride, *N,N*-dimethylformamide (DMF), methyl sul-

[†] This work was supported by NIH Grant GM55242 and a Pilot Research Project Award from the Cancer Center of the Albert Einstein College of Medicine. Z.-Y.Z. is a Sinsheimer Scholar.

* Address correspondence to these authors at 718-430-8641, dlawrenc@aecom.yu.edu (D.S.L.) and 718-430-4288, zyzzhang@aecom.yu.edu (Z.Y.Z.).

[‡] Department of Biochemistry.

[§] Department of Molecular Pharmacology.

^{||} These authors contributed equally to the work described herein.

foxide (DMSO), and diethyl ether were purchased from Aldrich in Sure/Seal bottles and were used as such. Benzo-triazole-1-yl-oxy-tris-(dimethylamino)-phosphonium hexafluorophosphate (BOP), *O*-(*N*-succinimidyl)-1,1,3,3-tetramethyluronium tetrafluoroborate (TSTU), and tetramethylfluoromamidinium hexafluorophosphate (TFFH) were purchased from Advanced Chemtech. All reactions were followed by TLC using E. Merck silica gel 60 F-254. Flash column chromatography was performed by using J. T. Baker silica gel (230–400 mesh). The structures of new compounds were characterized and confirmed by ^1H NMR (300 MHz), ^{13}C NMR (75 MHz), ^{31}P NMR (121.5 MHz), and ESI for mass spectral analysis. The final products were purified via preparative HPLC using three Waters radial compression modules (25 \times 10 cm) connected in series: gradient (solvent A: 0.1% TFA in water; solvent B: 0.1% TFA in acetonitrile) 0–3 min (100% A); a linear gradient from 3 to 5 min (90% A and 10% B); from 5 to 30 min (65% A and 35% B); a steep final gradient to 90% B for column cleansing purposes.

Benzyl 4-Formylcinnamate (5). 4-Formylcinnamic acid **4** (3.85 g, 0.022 mmol) was dissolved in CH_3OH (100 mL) and water (10 mL). The slurry solution was titrated to between pH 7 and 8 (pH paper) with a 20% aqueous solution of Cs_2CO_3 . The resulting homogeneous solution was stirred for 20 min at ambient temperature. The solvent was evaporated to dryness, giving solid cesium salt which was dried under high vacuum overnight. The solid was treated with benzyl bromide (5.62 g, 0.033 mmol) in DMF (60 mL). The slurry solution was stirred under a blanket of nitrogen overnight. The white solid was removed by filtration. The solvent was evaporated under vacuum to give yellow oil. The oil was taken up in ethyl acetate (100 mL), and it was filtered through a pad of Celite to remove the remaining solid impurities. The solvent was again evaporated, and the remaining oil was titrated with hexanes (30 mL). At this point, the desired product solidified. The solid was washed with hexanes (3 \times 10 mL) and dried under vacuum to give benzyl 4-formylcinnamate **5** (5.32 g, 91%): ^1H NMR (300 MHz, CDCl_3) δ 10.0 (s, 1H), 7.9 (d, J = 8.2 Hz, 2H), 7.7 (d, J = 16.0 Hz, 1H), 7.6 (d, J = 8.2 Hz, 2H), 7.4 (m, 5H), 6.6 (d, J = 16 Hz, 1H), 5.2 (s, 2H).

Synthesis of 6. Diethyl phosphite (0.11 g, 0.83 mmol) was added dropwise via a syringe to a suspension of sodium hydride (0.019 g, 0.79 mmol) in anhydrous THF (7 mL) at 0 °C (ice bath). The resulting slurry solution was stirred for 10 min. The ice bath was removed, and stirring was continued for another 30 min. The solution was then cooled to –78 °C (CO_2 /acetone) and transferred via a cannula to another flask containing a solution of benzyl 4-formylcinnamate **5** (0.21 g, 0.79 mmol) also at –78 °C. After the transfer was complete, the mixture solution was warmed to 0 °C, and stirring was continued for 1 h. The reaction was then quenched with a 10% aqueous solution of ammonium chloride (20 mL). The aqueous portion was separated and extracted with ethyl acetate (3 \times 30 mL). The combined organic layers were washed with brine (50 mL) and dried over sodium sulfate. Removal of solvent gave a yellow oil which was purified by flash column chromatography (SiO_2 , CH_2Cl_2 :EtOAc, 1:1) to afford pure product **6** (267 mg, 83%): ^1H NMR (300 MHz) δ 7.7 (d, J = 16 Hz, 1H), 7.5 (m, 4H), 7.4–7.3 (m, 5H), 6.5 (d, J = 16 Hz, 1H), 5.2 (s, 2H), 5.05 (d, J = 11 Hz, 1H), 4.07–4.03 (m, 4H), 1.3–1.2 (m, 6H).

Synthesis of 7. DMSO (0.072 g, 0.91 mmol) was added dropwise via a syringe to a solution of oxalyl chloride (0.10 g, 0.83 mmol) and CH_2Cl_2 (5 mL) at –78 °C. The resulting mixture was stirred for 10 min. Then a solution of **6** (0.167 g, 0.41 mmol) in CH_2Cl_2 (3 mL) was added dropwise. After another 15 min, the reaction mixture was treated with triethylamine (0.24 g, 2.4 mmol). The cold bath was removed, allowing the solution to warm to ambient temperature. The reaction solution was then poured into a separatory funnel containing water (60 mL). The aqueous portion was extracted with CH_2Cl_2 (3 \times 30 mL). The combined organic layers were washed with a 1% aqueous solution of HCl (4 \times 20 mL). Removal of solvent gave a yellow oil, which was dried under vacuum. The intermediate product was used without further purification and treated with diethylammonium sulfurtrifluoride (“DAST”) (**13**) (0.67 g, 4.13 mmol) at 0 °C. After 1 h, the ice bath was removed, and the mixture was stirred for another 2 h at room temperature. The solution was then diluted with CH_2Cl_2 (20 mL) and then slowly added to an ice cold saturated aqueous solution of sodium bicarbonate (50 mL). The aqueous portion was separated and extracted with CH_2Cl_2 (3 \times 20 mL). The combined organic layers were washed with brine and dried over Na_2SO_4 . Removal of solvent gave red oil which was purified by flash column chromatography (SiO_2 , CH_2Cl_2 :EtOAc, 9:1) to afford **7** (0.115 g, 66%): ^1H NMR (300 MHz, CDCl_3) δ 8.2 (d, J = 8.3 Hz, 2H), 7.7 (d, J = 16 Hz, 1H), 7.6 (d, J = 8.3 Hz, 2H), 7.4–7.3 (m, 5H), 6.5 (d, J = 16 Hz, 1H), 5.2 (s, 2H), 4.3 (quintet, J = 7.4 Hz, 4H), 1.3 (t, J = 7 Hz, 6H); ^{31}P NMR (121.5 MHz, CDCl_3) δ 13 (t, J = 115 Hz).

Synthesis of 8. 1,4-cyclohexadiene (0.36 g, 4.5 mmol) and Pd/C (10%) (100 mg) were added to a solution of **7** (115 mg, 0.27 mmol) in ethanol (5 mL). The resulting mixture was stirred at room temperature for 24 h. After the reaction was complete (TLC analysis), the solution was filtered through a pad of Celite to remove solid impurities. The solvent was evaporated to give compound **8** (90 mg, quantitative yield): ^1H NMR (300 MHz, CDCl_3) δ 10.7 (s, 1H), 7.5 (d, J = 7.7 Hz, 2H), 7.2 (d, J = 7.7 Hz, 2H), 4.2–4.0 (m, 4H), 2.9 (t, J = 7.6 Hz, 2H), 2.6 (t, J = 7.6 Hz, 2H), 1.2 (t, J = 7.0 Hz, 6H); ^{13}C NMR (300 MHz, CDCl_3) δ 177, 143, 130 (dt, J = 22 Hz, 14 Hz), 128, 126, 116 (dt, J = 263 Hz, 220 Hz), 65, 35, 30, 16; ^{31}P NMR (300 MHz, CDCl_3) δ 14 (t, J = 118 Hz).

Synthesis of Compound 9. The acid **8** (0.050 g, 0.149 mmol) in dry CH_2Cl_2 (1 mL) was treated with bis(trimethylsilyl)trifluoroacetamide (BSTFA) (200 μL , 0.754 mmol) at room temperature for 1 h and subsequently with bromotrimethylsilane (TMSBr) (300 μL , 2.273 mmol) overnight. After removal of most of the solvent by rotary evaporation, the residue was dissolved in water, washed with ether, and purified by HPLC to afford compound **9** (0.030 g, 72%). ^1H NMR (300 MHz, D_2O) δ 7.4 (d, J = 7.9 Hz, 2 H), 7.2 (d, J = 7.9 Hz, 2 H), 2.8 (t, J = 7.3 Hz, 2 H), 2.6 (t, J = 7.3 Hz, 2 H); ^{13}C NMR (75 MHz, D_2O) δ 178, 143, 132 (dt, J_1 = 13 Hz, J_2 = 22 Hz), 129, 126 (dt, J_1 = 1.3 Hz, J_2 = 6.8 Hz), 120 (dt, J_1 = 201 Hz, J_2 = 261 Hz), 35, 30; ^{19}F NMR (282 MHz, D_2O) δ –32 (d, J = 107 Hz); ^{31}P NMR (121.5 MHz, D_2O) δ 13 (t, J = 107 Hz); MS (ESI) calcd for $\text{C}_{10}\text{H}_{11}\text{F}_2\text{O}_5\text{P}$ 280.2, found 281.0.

Synthesis of Compound 10. The acid **8** (0.062 g, 0.184 mmol) was preactivated with TSTU (0.113 g, 0.375 mmol)

and diisopropylethylamine (DIEA) (65 μ L, 0.373 mmol) in 5 mL of DMF at room temperature for 10 min. Ammonium hydroxide (40 μ L, 0.592 mmol) was then added dropwise. After 20 min, most of the solvent was removed under vacuum and the mixture then extracted with CH_2Cl_2 (3 \times 40 mL)/water (20 mL). The combined organic phase was washed with brine and dried over Na_2SO_4 . Removal of solvent gave the crude phosphonodiester of compound **10** [^1H NMR (300 MHz, CDCl_3) δ 7.5 (d, J = 7.8 Hz, 2 H), 7.3 (d, J = 7.8 Hz, 2 H), 5.7 (d, 2 H), 4.3–4.0 (m, 4 H), 3.0 (t, J = 7.6 Hz, 2 H), 2.5 (t, J = 7.6 Hz, 2 H), 1.3 (t, J = 7.1 Hz, 6 H); ^{13}C NMR (75 MHz, CDCl_3) δ 175, 144 (d, J = 2.0 Hz), 131 (dt, J = 13.9, 20.6 Hz), 129, 127 (dt, J = 2.3, 1.2 Hz), 118 (dt, J = 220, 240 Hz), 65 (d, J = 6.8 Hz), 37, 31, 16 (d, J = 0.5 Hz); ^{19}F NMR (282 MHz, CDCl_3) δ –32 (d, J = 118 Hz); ^{31}P NMR (121.5 MHz, CDCl_3) δ 13.5 (t, J = 118 Hz) (0.050 g, 81%)], which (0.015 g, 0.044 mmol) was subsequently treated with excess iodotrimethylsilane (TMSI) (0.5 mL) in 1 mL of dry CH_2Cl_2 for 12 h at room temperature. The reaction mixture was then quenched with methanol, rotary evaporated to a semisolid, washed with ether, and purified by HPLC to afford compound **10** (0.009 g, 72%). ^1H NMR (300 MHz, D_2O) δ 7.4 (d, J = 7.9 Hz, 2 H), 7.2 (d, J = 7.9 Hz, 2 H), 2.8 (t, J = 7.2 Hz, 2 H), 2.5 (t, J = 7.2 Hz, 2 H); ^{13}C NMR (75 MHz, D_2O) δ 179, 143, 133 (dt, J = 1.3, 2.3 Hz), 129, 126 (dt, J = 2.1, 0.6 Hz), 121 (dt, J = 198, 260 Hz), 37, 31; ^{19}F NMR (282 MHz, D_2O) δ –35 (d, J = 105 Hz); ^{31}P NMR (121.5 MHz, D_2O) δ 11.6 (t, J = 105 Hz); MS (ESI) calcd for $\text{C}_{10}\text{H}_{12}\text{F}_2\text{NO}_4\text{P}$ 279.2, found 280.2.

Synthesis of General Structures 11 (Specific Example: Precursor to Compound 15). The acid **8** (0.035 g, 0.104 mmol) was activated with BOP reagent (0.070 g, 0.156 mmol) and NMM (0.031 g, 0.309 mmol) in acetonitrile (2 mL) [for the reaction with diaminobenzene (i.e., compounds **16–18**), TFFH was used as an activating reagent and DMF as solvent]. The resulting mixture was stirred at room temperature for 10 min. A solution of ethylenediamine (0.063 g, 1.05 mmol) in acetonitrile (1 mL) was then added. The reaction was complete in 30 min (TLC analysis). The solvent was removed under vacuum, and ethyl acetate (20 mL) and water (20 mL) were added to the crude product. The aqueous portion was extracted with ethyl acetate (3 \times 10 mL). The combined organic layers were washed with brine (20 mL) and dried over Na_2SO_4 . Purification was achieved by flash column chromatography (SiO_2 , CH_2Cl_2 : CH_3OH , 1:1 with 1% NH_4OH for alkylamine) to afford amine **11** (intermediate for compound **15**) (0.03 g, 76%) which was used subsequently in the next coupling reaction: ^1H NMR (300 MHz, CD_3OD) δ 7.6 (d, J = 8 Hz, 2H), 7.4 (d, J = 8 Hz, 2H), 4.4–4.2 (m, 4H), 3.4–3.3 (m, 2H), 3.1 (t, J = 7.5 Hz, 2H), 2.7 (t, J = 7.5 Hz, 2H), 2.5 (t, J = 7 Hz, 2H), 1.4 (t, J = 7 Hz, 6H).

Synthesis of General Structures 12 (Specific Example: Precursor to Compound 15). In a manner similar to the above procedure, acid **8** (0.27 mg, 0.079 mmol), BOP (0.70 g, 0.159 mmol), NMM (0.040 g, 0.40 mmol), and amine **11** (0.03 g, 0.079 mmol) gave dimer **12** (0.035 g, 63%) after purification by flash column chromatography (SiO_2 , CH_2Cl_2 : CH_3OH): ^1H NMR (300 MHz, CDCl_3) δ 7.7 (d, J = 8 Hz, 4H), 7.5 (d, J = 8 Hz, 4H), 6.5 (s, 2H), 4.5–4.3 (m, 8H), 3.5 (s,

4H), 3.2 (t, J = 7.5 Hz, 4H), 2.7 (t, J = 7.5 Hz, 4H), 1.5 (t, J = 7 Hz, 12H).

Synthesis of 13 (Compounds 14, 15, 17, 18; Specific Example: Compound 15). BSTFA (0.15 g, 0.6 mmol) was added at room temperature to a stirred solution of **12** (0.035 g, 0.05 mmol) in CH_2Cl_2 . After 30 min, the solution was cooled to –78 $^\circ\text{C}$, and TMSI (1.1 g, 0.5 mmol) was added via a syringe. The resulting mixture was stirred at –78 $^\circ\text{C}$ for 1 h and then at room temperature for 2 h. The solvent with excess TMSI was removed under reduced pressure. The crude product was then dissolved in 2 mL of acetonitrile containing water (10%) and TFA (1%). The resulting solution was stirred for 1 h. Removal of solvent gave a crude product which was purified by HPLC to afford pure compound **15** (5 mg, 17%): ^1H NMR (300 MHz, D_2O) δ 7.5 (d, J = 8 Hz, 4H), 7.3 (d, J = 8 Hz, 4H), 3.1 (s, 4H), 2.9 (t, J = 7.2 Hz, 4H), 2.5 (t, J = 7.1 Hz, 4H); ^{13}C NMR (75 MHz, D_2O) δ 176, 143, 132 (dt, J = 23, 12.4 Hz), 128, 126, 38, 37, 30; ^{31}P NMR (121.5 MHz, D_2O) δ 11 (t, J = 107 Hz); MS (ESI) calcd for $\text{C}_{22}\text{H}_{26}\text{O}_8\text{F}_4\text{P}_2\text{N}_2$ 584.5, found 586.0.

Compound 14: ^1H NMR (300 MHz, D_2O) δ 7.5 (d, J = 7.9 Hz, 4H), 7.3 (d, J = 7.9 Hz, 4H), 3.0 (t, J = 7.3 Hz, 4H), 2.6 (t, J = 7.9 Hz, 4H); ^{13}C NMR (75 MHz, D_2O) δ 175, 143, 132 (dt, J = 22.2, 12.6 Hz), 128, 126, 120 (m), 35, 30; ^{31}P NMR (121.5 MHz, D_2O) δ 11.5 (t, J = 106 Hz); MS (ESI) calcd for $\text{C}_{20}\text{H}_{22}\text{O}_8\text{F}_4\text{P}_2\text{N}_2$ 556.4, found 557.0.

Compound 17: ^1H NMR (300 MHz, D_2O) δ 7.4 (d, J = 8 Hz, 4H), 7.2 (d, J = 8 Hz, 4H), 7.1 (t, J = 7.9 Hz, 1H), 7.0 (s, 1H), 6.9 (d, 7.9 Hz, 2H), 2.8 (t, J = 6.9 Hz, 4H), 2.5 (t, J = 6.9 Hz, 4H); ^{13}C NMR (75 MHz, D_2O) δ 174, 143, 137, 132 (dt, J = 32, 12.4 Hz), 130, 129, 126, 118, 115, 38, 31; ^{31}P NMR (121.5 MHz, D_2O) δ 11 (t, J = 107 Hz); MS (ESI) calcd for $\text{C}_{26}\text{H}_{26}\text{O}_8\text{F}_4\text{P}_2\text{N}_2$, 632.6; found 633.2.

Compound 18: ^1H NMR (300 MHz, D_2O) δ 7.5 (d, J = 7.9 Hz, 4H), 7.3 (d, J = 7.9 Hz, 4H), 7.25–7.20 (m, 2H), 7.1–7.0 (m, 2H), 2.9 (t, J = 6.8 Hz, 4H), 2.6 (t, J = 6.8 Hz, 4H); ^{13}C NMR (75 MHz, D_2O) δ 175, 143, 132 (m), 130, 129, 128, 127, 126, 37, 31; ^{31}P NMR (121.5 MHz, D_2O) δ 11.6 (t, J = 107 Hz); MS (ESI) calcd for $\text{C}_{26}\text{H}_{26}\text{O}_8\text{F}_4\text{P}_2\text{N}_2$ 632.6, found 633.2.

Direct Synthesis of General Structure 13 (Compounds 16, 19, 20, 39, and 40). The appropriate equimolar concentration of acid **8** was reacted with the specific di- or triamine by the above-mentioned BOP/NMM procedure to directly give the corresponding dimer or trimer of general structure **12** in the solution. The latter was then diluted with EtOAc, washed with water or dilute HCl, evaporated to dryness, treated with TMSI and purified by HPLC to afford compounds **16**, **19**, **20**, **39**, and **40**.

Compound 16: ^1H NMR (300 MHz, D_2O) δ 7.4 (d, J = 7.9 Hz, 4 H), 7.2 (d, J = 7.9 Hz, 4 H), 7.1 (s, 4 H), 2.9 (t, J = 7.2 Hz, 4 H), 2.5 (t, J = 7.2 Hz, 4 H); ^{13}C NMR (75 MHz, D_2O) δ 175, 134, 129, 128, 126 (m), 125, 123, 122 (m), 32, 30; ^{19}F NMR (282 MHz, D_2O) δ –35 (d, J = 105 Hz); ^{31}P NMR (121.5 MHz, D_2O) δ 11.6 (t, J = 105 Hz); MS (ESI) calcd for $\text{C}_{26}\text{H}_{26}\text{F}_4\text{N}_2\text{O}_8\text{P}_2$ 632.4, found 633.0.

Compound 19: ^1H NMR (300 MHz, D_2O) δ 7.3 (d, J = 7.9 Hz, 4 H), 7.2 (d, J = 7.9 Hz, 4 H), 6.7 (s, 4 H), 4.0 (s, 4 H), 2.9 (t, J = 7.0 Hz, 4 H), 2.6 (t, J = 7.0 Hz, 4 H); ^{13}C NMR (75 MHz, D_2O) δ 175, 143, 137, 133, 129, 127, 126 (m), 122 (m), 43, 38, 31; ^{19}F NMR (282 MHz, D_2O) δ –35

(d, $J = 105$ Hz); ^{31}P NMR (121.5 MHz, D_2O) δ 11.6 (t, $J = 105$ Hz); MS (ESI) calcd for $\text{C}_{28}\text{H}_{30}\text{F}_4\text{N}_2\text{O}_8\text{P}_2$ 660.5, found 661.8.

Compound 20: ^1H NMR (300 MHz, D_2O) δ 7.3 (d, $J = 7.8$ Hz, 4 H), 7.16 (d, $J = 7.8$ Hz, 4 H), 7.08 (t, $J = 7.6$ Hz, 1H), 6.74 (s, 1H), 6.70 (d, $J = 7.6$ Hz, 2H), 4.0 (s, 4H), 2.8 (t, $J = 6.9$ Hz, 4 H), 2.5 (t, $J = 6.9$ Hz, 4 H); ^{13}C NMR (75 MHz, D_2O) δ 176, 143, 138, 129, 128.9, 128.8, 127–126 (m), 121 (m), 43, 37, 32; ^{19}F NMR (282 MHz, D_2O) δ –35 (d, $J = 106$ Hz); ^{31}P NMR (121.5 MHz, D_2O) δ 11.5 (t, $J = 106$ Hz); MS (ESI) calcd for $\text{C}_{28}\text{H}_{30}\text{F}_4\text{N}_2\text{O}_8\text{P}_2$ 660.5, found 662.2.

Compound 39: ^1H NMR (300 MHz, D_2O) δ 7.5 (t, 6 H), 7.3 (t, 6 H), 3.1 (s, 4 H), 3.0 (t, $J = 5.5$ Hz, 2 H), 2.9 (m, 8 H), 2.5 (m, 6 H); ^{13}C NMR (75 MHz, D_2O) δ 176.1, 175.9, 175.8, 143.4, 143.1, 133–132 (m), 129, 126 (m), 121 (m), 120 (m), 48, 45, 38–37 (m), 34, 31.2, 31.1; ^{19}F NMR (282 MHz, D_2O) δ –32.3 (d, $J = 106$ Hz), –32.4 (d, $J = 106$ Hz); ^{31}P NMR (121.5 MHz, D_2O) δ 11.6 (t, $J = 106$ Hz); MS (ESI) calcd for $\text{C}_{34}\text{H}_{40}\text{F}_6\text{N}_3\text{O}_{12}\text{P}_3$ 889.6, found 890.2.

Compound 40: ^1H NMR (300 MHz, D_2O) δ 7.5 (d, $J = 7.8$ Hz, 6 H), 7.3 (d, $J = 7.8$ Hz, 6 H), 3.1 (t, $J = 5.7$ Hz, 6 H), 3.0 (t, $J = 6.9$ Hz, 6 H), 2.9 (t, $J = 5.7$ Hz, 6 H), 2.6 (t, $J = 6.9$ Hz, 6 H); ^{13}C NMR (75 MHz, D_2O) δ 177, 143, 133, 129, 126 (m), 122 (m), 54, 37, 35, 31; ^{19}F NMR (282 MHz, D_2O) δ –32 (d, $J = 106$ Hz); ^{31}P NMR (121.5 MHz, D_2O) δ 11.6 (t, $J = 106$ Hz); MS (ESI) calcd for $\text{C}_{36}\text{H}_{45}\text{F}_6\text{N}_4\text{O}_{12}\text{P}_3$ 932.7, found 933.8.

Synthesis of Compound 22. To a solution of phenyliodosyl bis(trifluoroacetate) (Loudon et al., 1984) (0.090 g, 0.21 mmol) in 0.3 mL of acetonitrile and 0.3 mL of water was added the phosphonodiester of compound **10** (0.015 g, 0.045 mmol), and the resultant mixture was stirred at room temperature for 6 h. The solution was then diluted with 2 mL of water, and 1 mL of concentrated HCl was subsequently added. Extraction with 3×6 mL ether and evaporation of the combined organics after drying furnished essentially pure *p*-diethylphosphonodifluoromethyl phenylethylamine (hydrochloride salt) ^1H NMR (300 MHz, D_2O) δ 7.6 (d, $J = 7.9$ Hz, 2 H), 7.5 (d, $J = 7.9$ Hz, 2 H), 4.3 (quintet, 4H), 3.3 (t, $J = 7.5$ Hz, 2 H), 3.1 (t, $J = 7.5$ Hz, 2 H), 1.3 (t, $J = 7.1$ Hz, 6 H); ^{13}C NMR (75 MHz, D_2O) δ 141, 130.1 (dt, $J = 13.7, 20.6$ Hz), 129.5, 127 (dt, $J = 2.5, 4.6$ Hz), 118 (dt, $J = 222, 252$ Hz), 67 (d, $J = 7.2$ Hz), 40, 33, 16 (d, $J = 5.2$ Hz); ^{19}F NMR (282 MHz, D_2O) δ –33 (d, $J = 122$ Hz); ^{31}P NMR (121.5 MHz, D_2O) δ 14.6 (t, $J = 122$ Hz) (0.012 g, 75%). The acid **8** (0.045 g, 0.134 mmol) was then coupled to the *p*-diethylphosphonodifluoromethyl phenylethylamine (hydrochloride salt) (0.050 g, 0.146 mmol) after preactivation by TSTU (0.080 g, 0.266 mmol) and phenyliodosyl bis(trifluoroacetate) (70 μL , 0.402 mmol) in 2 mL of DMF for 10 min at room temperature. After 5 h, most of the solvent was removed under vacuum, and the mixture was extracted with EtOAc (3×10 mL)/water (10 mL). The combined organic phase was washed with brine and dried over Na_2SO_4 . Removal of solvent and further purification by flash column chromatography (10% MeOH in EtOAc) gave the phosphonotetraester of compound **22** [^1H NMR (300 MHz, CDCl_3) δ 7.5 (d, $J = 7.9$ Hz, 4 H), 7.3 (d, $J = 7.9$ Hz, 2 H), 7.2 (d, $J = 7.9$ Hz, 2 H), 5.5 (t, 1H), 4.2 (m, 8 H), 3.5 (q, 2 H), 3.0 (t, $J = 7.1$ Hz, 2 H), 2.8 (t, $J = 6.7$ Hz, 2 H), 2.4 (t, $J = 7.1$ Hz, 2 H), 1.3 (m, 12 H);

^{13}C NMR (75 MHz, CDCl_3) δ 172, 144, 142, 132–130 (m), 129.03, 129.02, 128.73, 128.72, 127–126 (m), 121 (m), 118 (m), 65.07, 65.02, 64.98, 64.94, 41, 38, 36, 32; ^{19}F NMR (282 MHz, CDCl_3) δ –32.3 (d, $J = 117$ Hz), –32.4 (d, $J = 117$ Hz); ^{31}P NMR (121.5 MHz, CDCl_3) δ 13.7 (t, $J = 117$ Hz), 7.5 (t, $J = 117$ Hz)] (0.065 g, 78%). The ethylester protecting groups were removed via treatment with excess TMSBr (0.5 mL) in 1 mL of dry CH_2Cl_2 overnight at room temperature. Extraction with ether and purification of the aqueous phase by HPLC furnished compound **22** (0.006 g, 10%). ^1H NMR (300 MHz, D_2O) δ 7.4 (t, 4 H), 7.2 (d, $J = 8.0$ Hz, 2 H), 7.1 (d, $J = 8.1$ Hz, 2 H), 3.3 (t, $J = 6.7$ Hz, 2 H), 2.8 (t, $J = 7.1$ Hz, 2 H), 2.6 (t, $J = 6.7$ Hz, 2 H), 2.4 (t, $J = 7.1$ Hz, 2 H); ^{13}C NMR (75 MHz, D_2O) δ 176, 144, 142, 133 (m), 130, 129, 127 (m), 121 (m), 117 (m), 41, 38, 35, 32; ^{19}F NMR (282 MHz, D_2O) δ –32.3 (d, $J = 106$ Hz), –32.4 (d, $J = 106$ Hz); ^{31}P NMR (121.5 MHz, D_2O) δ 11.6 (t, $J = 106$ Hz); MS (ESI) calcd for $\text{C}_{19}\text{H}_{21}\text{F}_4\text{NO}_7\text{P}_2$ 513.3, found 513.8.

Synthesis of 26. Sodium hydride (0.127 g, 5.29 mmol) was added in several portions to a solution of catechol (0.265 g, 2.4 mmol) in anhydrous DMF (10 mL) at ambient temperature. The resulting suspension was stirred for 30 min. Methyl 4-(bromomethyl)benzoate **25** (1.21 g, 5.29 mmol) was added in one portion. The reaction was complete in 3 h (TLC analysis). The solvent was then removed under vacuum, and the recovered residue was dissolved in ethyl ether (50 mL) and water (50 mL). The aqueous portion were separated and then extracted with ether (3×30 mL). The combined organic extracts was washed with brine (50 mL) and dried over Na_2SO_4 . Purification was achieved by flash column chromatography (SiO_2 , hexanes:ethyl acetate, 2:1) to afford compound **26** as a white solid (0.8 g, 82%): ^1H NMR (500 MHz, CDCl_3) δ 8.0 (d, $J = 8.2$ Hz, 4H), 7.5 (d, $J = 8.2$ Hz, 4H), 6.9 (m, 4H), 5.2 (s, 4H), 3.9 (s, 6H); ^{13}C NMR (75 MHz, CDCl_3) δ 167, 148, 142, 129.8, 129.5, 126, 121, 114, 70, 52.

Synthesis of 27. LiBH_4 (45 mg, 2.15 mmol) was added in one portion to a solution of ester **26** (0.21 g, 0.51 mmol) in anhydrous THF (15 mL) and methanol (0.1 mL). The mixture was heated to reflux for 3 h and then cooled to room temperature. Ice cold water (50 mL) was slowly added to destroy the excess LiBH_4 . The aqueous portion was separated and then extracted with ethyl acetate (3×30 mL). The combined organic layers were washed with brine and dried over Na_2SO_4 . Removal of solvent gave the alcohol intermediate as a white solid (quantitative yield) which was used without further purification: ^1H NMR (500 MHz, CDCl_3) δ 7.4 (d, $J = 8$ Hz, 4H), 7.3 (d, $J = 8$ Hz, 4H), 6.9 (m, 4H), 5.1 (s, 4H), 4.6 (s, 4H); ^{13}C NMR (75 MHz, CDCl_3) δ 149, 140, 136, 127.5, 127, 121, 115, 71, 65.

The oxidation of the alcohol derivative was conducted according to the procedure described previously (see preparation of **7**). Oxalyl chloride (0.32 g, 2.55 mmol), DMSO (0.32 g, 4.1 mmol), alcohol intermediate (0.18 g, 0.5 mmol), and Et_3N (1 mL) gave aldehyde **27** (>95% yield): ^1H NMR (500 MHz, CDCl_3) δ 10 (s, 2H), 7.8 (d, $J = 8$ Hz, 4H), 7.6 (d, $J = 8$ Hz, 4H), 6.9 (s, 4H), 5.2 (s, 4H); ^{13}C NMR (75 MHz, CDCl_3) δ 192, 148, 144, 135, 129, 127, 121, 115, 70.

Synthesis of 28. Diethyl phosphite (0.06 g, 0.43 mmol) was added dropwise via a syringe to a suspension of sodium hydride (0.010 g, 0.43 mmol) in anhydrous THF (5 mL) at

0 °C (ice bath). The resulting slurry solution was stirred for 10 min, the ice bath was removed, and stirring then continued for an additional 30 min. The solution was recooled to 0 °C and transferred, via a cannula, to a flask containing a solution of **27** (0.050 g, 0.144 mmol) which was also at 0 °C. After the transfer was complete, the mixture was stirred for 1 h and then quenched with a 10% aqueous solution of ammonium chloride (20 mL). The aqueous portion was separated and extracted with ethyl acetate (3 × 20 mL). The combined organic layers were washed with brine (30 mL) and dried over sodium sulfate. Removal of solvent gave yellow oil **28** (0.083 g, 93%) which was subsequently oxidized.

Synthesis of 29 and Subsequent Deprotection to Furnish 23. The oxidation of **28** was carried out according to the method described previously (see preparation of **7**). Compound **28** (0.083 g, 0.134 mmol), oxalyl chloride (0.1 g, 0.86 mmol), DMSO (0.1 g, 1.3 mmol), and Et₃N (0.3 mL) gave the carbonyl intermediate in quantitative yield: ¹H NMR (300 MHz, CDCl₃) δ 8.2 (d, *J* = 8.3 Hz, 4H), 7.5 (d, *J* = 8.3 Hz, 4H), 6.88 (m, 4H), 5.2 (s, 4H), 4.2 (quintet, *J* = 7.1 Hz, 8H), 1.3 (t, *J* = 7 Hz, 12H); ³¹P (121.5 MHz, CDCl₃) δ 0 (s); ¹³C NMR (75 MHz) δ 198 (d, 175.4 Hz), 148, 144, 135 (d, 63 Hz), 130, 127, 122, 114, 70, 64 (d, 7.3 Hz), 16. The intermediate was treated with DAST (1.34 mmol) at 0 °C. After 1 h, the ice bath was removed and the mixture stirred for 4 h at room temperature. Aqueous workup was carried out as described previously (see preparation of **7**). Removal of solvent gave a red oil which was purified by flash column chromatography (SiO₂, CH₂Cl₂:CH₃OH, 9:1) to afford **29** which was treated with excess bromotrimethylsilane (TMSBr) (1 mL). The solution was stirred overnight. The TMSBr was evaporated to give white solid and the solid, was then dissolved in methanol (5 mL) and water (3 mL). The solution was stirred at ambient temperature for 30 min. The solvent was again evaporated to give a red oil which was purified by HPLC to afford **23** (18 mg, 24%): ¹H NMR (300 MHz, D₂O) δ 7.5 (d, *J* = 8.1 Hz, 4H), 7.4 (d, *J* = 8.1 Hz, 4H), 6.96–6.93 (m, 2H), 6.83–6.79 (m, 2H), 5.1 (s, 4H); ³¹P NMR (121.5 MHz, D₂O) δ 5.3 (t, *J* = 105.6 Hz); ¹³C NMR (75 MHz, D₂O) δ 150, 141, 128, 127.7, 127.6, 123, 116, 71. MS (ESI) calcd for C₂₂H₂₀F₄O₈P₂ 550.3, found 551.0.

Synthesis of 30. Compound **30** was prepared in a fashion analogous to that shown in Scheme 2, namely via a two-step protocol. Acid **8** (20 mg, 0.059 mmol) was activated with TFFH (17 mg, 0.065 mmol) and DIEA (0.03 g, 23 mmol) in DMF (1 mL). After the mixture was stirred for 20 min at ambient temperature, a solution of 1,3-diaminobenzoic acid (18 mg, 0.118 mmol) in DMF (1 mL) was added. The reaction was complete in 1 h (TLC analysis). The solvent was removed under vacuum. The recovered residue was dissolved in ethyl acetate (20 mL) and H₂O (20 mL). The aqueous portion was extracted with ethyl acetate (3 × 10 mL), and the combined organic layers were washed with brine and dried over Na₂SO₄. Purification was achieved by flash column chromatography (SiO₂, CH₂Cl₂:CH₃OH, 1:4) to afford yellow oil (monosubstituted 1,3-diaminobenzoic acid) which was used subsequently: ¹H NMR (300 MHz, CD₃OD) δ 7.5 (d, *J* = 8 Hz, 2H), 7.43 (d, *J* = 8 Hz, 2H), 7.4 (s, 1H), 7.2 (s, 1H), 7.1 (s, 1H), 4.1 (m, 4H), 3.1 (t, *J* = 7.2 Hz, 2H), 2.7 (t, *J* = 7.1 Hz, 2H), 1.2 (t, *J* = 7 Hz, 6H).

The monosubstituted product was converted to the desired disubstituted species in a manner similar to that just described using acid **8** (20 mg, 0.059 mmol), TFFH (17 mg, 0.065 mmol), and DIEA (0.03 g, 23 mmol) to give dimer **30** (40 mg, 85%) after purification: ¹H NMR (300 MHz, CD₃OD) δ 8.05 (s, 1H), 7.9 (s, 2H), 7.5 (d, *J* = 7.9 Hz, 4H), 7.4 (d, *J* = 7.9 Hz, 4H), 4.1–4.0 (m, 8H), 3.0 (t, *J* = 7 Hz, 4H), 2.7 (t, *J* = 7 Hz, 4H), 1.2 (t, *J* = 7 Hz, 12H).

Conversion of 30 to Compounds 21, 32–38. Compound **30** (30 mg, 0.038 mmol) was activated with TSTU (30 mg, 0.11 mmol) and NMM (0.05 mL) in DMF at ambient temperature. After 30 min (TLC analysis), the solvent was evaporated to give an oily residue which was dissolved in ethyl acetate (20 mL) and H₂O (20 mL). The aqueous portion was extracted with ethyl acetate (3 × 10 mL). The combined organic layers were washed with water (15 mL), and brine (15 mL) and dried over Na₂SO₄. Removal of solvent gave the activated ester intermediate **31** which was dried under vacuum. This compound was used without further purification. The deprotection of **31** was carried out by the method described previously (see synthesis of **13**). Compound **31** (15 mg, 0.017 mmol), BSTFA (0.17 g, 0.68 mmol), and TMSI (0.11 g, 0.54 mmol) gave **31** which was used without further purification. Appropriate amines (5 molar equiv) and NMM (15–20 molar equiv) were separately added to a solution of **31** in DMF (3 mL). The mixtures were stirred for 5 h. The solvent from the reactions was evaporated under vacuum to give oily residues. Purification was achieved by HPLC to afford desired trimers (20–30%).

Compound 21: ¹H NMR (300 MHz, CD₃OD) δ 7.43 (s, 2H), 7.42 (s, 1H), 7.3 (d, *J* = 7.8 Hz, 4H), 7.0 (d, *J* = 7.8 Hz, 4H), 2.7 (t, *J* = 6.9 Hz, 4H), 2.4 (t, *J* = 6.8 Hz, 4H); ³¹P NMR (121.5 MHz, D₂O) δ 5.5 (t, *J* = 108 Hz); ¹³C NMR (75 MHz, D₂O) δ 215, 173, 168, 142, 137, 131, 130, 128, 126, 118, 38, 31. MS (ESI) calcd for C₂₇H₂₆F₄N₂O₁₀P₂ 676.5, found 677.0.

Compound 32: ¹H NMR (300 MHz, D₂O) δ 7.4 (d, *J* = 7.9 Hz, 4 H), 7.32 (d, *J* = 1.7 Hz, 2 H), 7.30 (d, *J* = 7.9 Hz, 4 H), 7.1 (s, 1 H), 3.3 (t, *J* = 6 Hz, 2 H), 2.9 (t, *J* = 6.9 Hz, 4 H), 2.7 (t, *J* = 6.9 Hz, 4 H), 2.3 (t, *J* = 6 Hz, 2 H), 1.57–1.55 (m, 4 H); ³¹P NMR (121.5 MHz, D₂O) δ 5.4 (t, *J* = 106 Hz). MS (ESI) calcd for C₃₂H₃₅F₄N₃O₁₁P₂ 775.6, found 776.2.

Compound 33: ¹H NMR (300 MHz, D₂O) δ 8.0 (d, *J* = 19 Hz, 1 H), 7.95 (d, *J* = 7.5 Hz, 1 H), 7.87 (m, 1 H), 7.7–7.5 (m, 8 H), 7.4 (d, *J* = 1.7 Hz, 2 H), 7.3 (d, *J* = 7.9 Hz, 4 H), 7.2 (t, *J* = 1.7 Hz, 1 H), 5.0 (s, 2 H), 3.0 (t, *J* = 6.9 Hz, 4 H), 2.7 (t, *J* = 6.9 Hz, 4 H); ³¹P NMR (121.5 MHz, D₂O) δ 5.4 (t, *J* = 105 Hz); MS (ESI) calcd for C₃₈H₃₅F₄N₃O₉P₂ 815.7, found 816.2.

Compound 34: ¹H NMR (300 MHz, D₂O) δ 7.4 (d, *J* = 7.9 Hz, 4H), 7.3–7.2 (m, 6H), 7.1 (s, 1H), 3.8 (m, 1H), 3.0 (t, *J* = 6.9 Hz, 4H), 2.7 (t, *J* = 6.9 Hz, 4H), 2.6 (m, 1H), 1.97–1.90 (m, 2H), 1.70–1.59 (m, 6H); ³¹P NMR (121.5 MHz, D₂O) δ 5.4 (t, *J* = 105 Hz). MS (ESI) calcd for C₃₄H₃₇F₄N₃O₁₁P₂ 801.6, found 802.2.

Compound 35: ¹H NMR (300 MHz, D₂O) δ 7.5 (d, *J* = 7.9 Hz, 4 H), 7.4 (d, *J* = 7.9 Hz, 4 H), 7.3 (d, *J* = 1.7 Hz, 2 H), 7.2 (m, 3 H), 6.9 (d, *J* = 8.5 Hz, 2 H), 3.6 (t, *J* = 6.5 Hz, 2 H), 3.1 (t, *J* = 7.3 Hz, 4 H), 2.9 (t, *J* = 6.5 Hz, 2 H), 2.8 (t, *J* = 7.3 Hz, 4 H); ³¹P NMR (121.5 MHz, D₂O) δ 5.4

(t, $J = 105$ Hz); MS (ESI) calcd for $C_{35}H_{35}F_4N_3O_{10}P_2$ 795.6, found 796.2.

Compound 36: 1H NMR (300 MHz, D_2O) δ 7.85 (s, 2 H), 7.80 (d, $J = 8.6$ Hz, 2 H), 7.50–7.42 (m, 7 H), 7.27 (d, $J = 7.8$ Hz, 4 H), 4.6 (s, 2 H), 3.0 (t, $J = 6.5$ Hz, 4 H), 2.7 (t, $J = 6.5$ Hz, 4 H); ^{31}P NMR (121.5 MHz, D_2O) δ 6.5 (t, $J = 94$ Hz). MS (ESI) calcd for $C_{34}H_{34}F_4N_4O_{11}P_2S$ 844.7, found 845.2.

Compound 37: 1H NMR (300 MHz, D_2O) δ 7.97 (s, 2 H), 7.87 (s, 1 H), 7.7 (m, 3 H) 7.55 (d, $J = 7.9$ Hz, 4 H), 7.35 (d, $J = 7.9$ Hz, 4 H), 4.7 (s, 2 H), 3.1 (t, $J = 6.9$ Hz, 4 H), 2.7 (t, $J = 6.9$ Hz, 4 H). MS (ESI) calcd for $C_{36}H_{31}F_{10}N_3O_9P_2$ 901.6, found 902.0.

Compound 38: 1H NMR (300 MHz, D_2O) δ 7.8 (d, $J = 8.1$ Hz, 2 H), 7.4 (d, $J = 7.9$ Hz, 4 H), 7.38 (s, 2 H), 7.3 (d, $J = 8.1$ Hz, 2 H), 7.26 (d, $J = 7.9$ Hz, 4 H), 7.2 (s, 1 H), 4.5 (s, 2 H), 2.9 (t, $J = 7.2$ Hz, 4 H), 2.6 (t, $J = 7.2$ Hz, 4 H); ^{31}P NMR (121.5 MHz, D_2O) δ 5.5 (t, $J = 108$ Hz). MS (ESI) calcd for $C_{35}H_{33}F_4N_3O_{11}P_2$ 809.6, found 810.2.

Recombinant PTP1B, LAR, PTP α , and VHR. The cDNA encoding the catalytic domain of human PTP1B (amino acids 1–321) was obtained using the polymerase chain reaction (PCR) from a human fetal brain cDNA library (Stratagene). The PCR primers used were 5'-AGCTGGATCCATATG-GAGATGGAAA AGGAGTT (encoding both a *Bam*HI and a *Nde*I site), and 3'-ACGCGAATTCTTAATTGTGTGG CTCCAGGATTCG (encoding an *Eco*RI site). The PCR product was digested with *Bam*HI and *Eco*RI and subcloned into a pUC118 vector. The PTP1B coding sequence was confirmed by DNA sequencing. The coding region for PTP1B was then cut from pUC118–PTP1B with *Nde*I and *Eco*RI and ligated to the corresponding sites of plasmid pT7–7. The PTP1B coding sequence was placed in frame downstream of the phage T7 RNA polymerase promoter at the *Nde*I site of pT7–7 to provide the translational initiation at Met 1 of PTP1B. The resulting plasmid pT7–7/PTP1B was used to transform *Escherichia coli* BL21(DE3). The expression and purification of the recombinant PTP1B is described in ref 12. Recombinant PTP1, the rat structural homologue of human PTP1B, was expressed and purified, as described previously (14). The pGEX plasmid containing the coding sequence for both of the PTPase domain of human PTP α was a generous gift from Dr. Frank Jirik of the University of British Columbia. The recombinant glutathione S-transferase (GST) fusion protein was purified, and the intracellular fragment of PTP α containing both of the PTPase domains was cleaved off the fusion protein as described (15). Recombinant LAR containing both PTPase domains were purified as described (16). Recombinant VHR dual specificity phosphatase was purified to homogeneity according to a published procedure (17).

PTPase Assay with *p*-Nitrophenyl Phosphate as a Substrate. The phosphatase activity was assayed at 25 °C in a reaction mixture (0.2 mL) containing appropriate concentrations of *p*-nitrophenyl phosphate (pNPP) as substrate. The buffer used was pH 7.0, 50 mM 3,3-dimethylglutarate, 1 mM EDTA. The ionic strength of the solution was adjusted using NaCl to $I = 0.15$ M. The reaction was initiated by addition of enzyme and quenched after 2–3 min by addition of 1 mL of 1 N NaOH. The nonenzymatic hydrolysis of the substrate was corrected by measuring the optical density of the control without the addition of enzyme. The amount of

product *p*-nitrophenol was determined from the absorbance at 405 nm using a molar extinction coefficient of $18\,000\text{ M}^{-1}\text{cm}^{-1}$ (18). Steady state kinetic parameters were evaluated by fitting directly the v vs $[S]$ data to the Michaelis–Menten equation using KINETASYST (IntelliKinetics, State College, PA).

PTPase Assay with a *p*Tyr-Containing Peptide as a Substrate. A synthetic tris-phosphotyrosyl dodecapeptide (TRDIPYETDpYpYRK–NH₂) corresponding to the amino acid sequence 1142–1153 of the kinase activation loop of the insulin receptor was used as a more physiologically relevant substrate. All assays were performed at 25 °C in pH 7, 50 mM 3,3-dimethylglutarate, 1 mM EDTA, ionic strength of 0.15 M buffer. A continuous spectrophotometric assay described previously was employed to determine k_{cat} and K_m (19) for the pTyr-containing peptide. The dephosphorylation reaction was monitored by the increase in fluorescence at 305 nm. Fluorometric determinations were performed on a Perkin-Elmer LS50B fluorometer which was equipped with a water-jacketed cell holder, permitting maintenance of the reaction mixture at the desired temperature.

Determination of Inhibition Constant (K_i). Inhibition constants for the PTPase inhibitors were determined for PTP1B, LAR, PTP α , and VHR in the following manner. The initial rate at eight different substrate concentration concentrations ($0.2 K_m$ to $5 K_m$) was measured at three different fixed inhibitor concentrations (11). The inhibition constant was obtained, and the inhibition pattern was evaluated using a direct curve-fitting program KINETASYST (IntelliKinetics, State College, PA).

RESULTS AND DISCUSSION

The propagation and termination of signaling events controlling many cellular processes are determined by the level of tyrosine phosphorylation. The phosphorylation level, in turn, is maintained in an exquisite balance by the reciprocal activities of protein-tyrosine kinases and phosphatases. The PTPase family is presently comprised of approximately 100 enzymes which can be either receptor-like or cytoplasmic. Membership to this family of enzymes requires the presence of the PTPase signature motif, (H/V)CX₅R(S/T), housed within the catalytic domain (2). The receptor-like PTPases, exemplified by LAR (leukocyte common antigen-related) and PTP α , generally have an extracellular domain, a single transmembrane region, and one or two cytoplasmic PTPase domains. The intracellular PTPases, exemplified by PTP1B, contain a single catalytic domain and various amino or carboxyl terminal extensions including SH2 domains that may have targeting or regulatory functions. Interestingly, based on the similar biochemical and structural properties, the PTPase superfamily also includes the dual specificity phosphatases, such as VHR (20) and cdc25 phosphatases, that can utilize protein substrates containing phosphotyrosine, as well as phosphoserine and phosphothreonine (21).

Several PTPases, including LAR, PTP α , and PTP1B, have been implicated in the insulin-mediated signal transduction pathway (4). All three PTPases are considered to be negative regulators of insulin action. For example, high intracellular concentrations of LAR reduce the ability of insulin-sensitive cells to respond to insulin (22). Furthermore, all three enzymes appear to either associate with and/or catalyze the dephosphorylation (and inactivation) of the insulin receptor

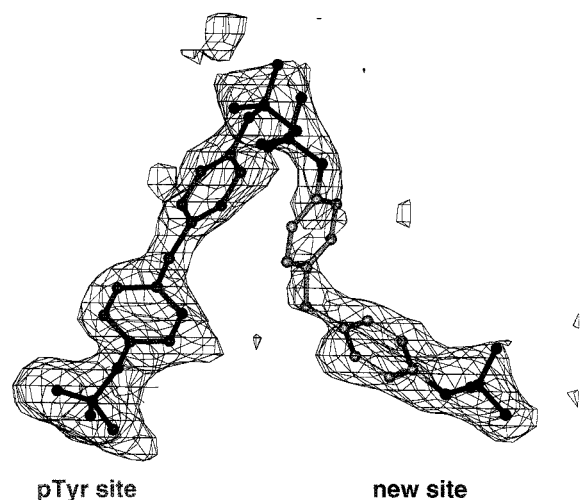


FIGURE 1: PTP1B contains two adjacent aryl phosphate binding sites, one at the active site and the other at a proximal noncatalytic site (12). Compound **1** binds to these two sites in a mutually exclusive fashion, whereas phosphotyrosine is simultaneously accommodated in both sites. The structure presented is of compound **1** bound to the PTP1B/C215S catalytically inactive mutant.

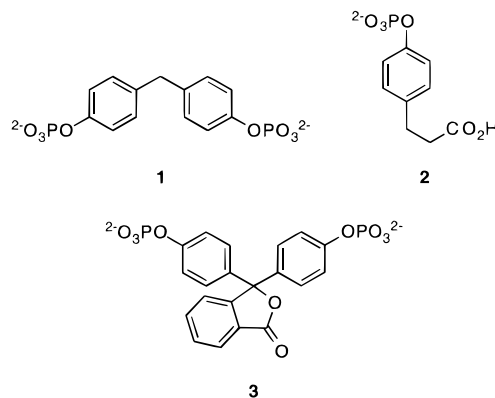
(IR) (23–27). Indeed, there now exists a body of evidence which suggests that one or more of these PTPases play a pivotal role in the pathogenesis of insulin resistance (6, 27–28). We describe herein highly selective PTP1B inhibitors that exhibit little or no activity against PTP α , LAR, or the dual specificity PTPase VHR.

Many of the PTPase inhibitors that have been identified to date, such as vanadate, tend to exhibit broad activity against a multitude of phosphatase targets. Several recent reports have focused on the design of novel PTPase inhibitors, with the ultimate goal being the acquisition of potent, yet highly selective agents. Burke and his colleagues have shown that the aryl phosphate group in PTPase substrates can be replaced with a hydrolytically resistant difluorophosphonate moiety to produce effective PTPase inhibitors (29–32). Several tripeptide-cinnamic acid conjugates were reported to exhibit K_i values of under 100 nM against PTP1B (33). However, the electrophilic nature of the cinnamic acid moiety does raise the possibility that these species serve as affinity labels rather than simple reversible inhibitors. In the area of covalent modifying agents, α -halobenzylphosphonates have been recently shown to rapidly inactivate the *Yersinia* PTPase (34). Finally, there have been several examples of nonpeptidic reversible inhibitors of PTPases. Perhaps the most notable is the recent report of oxazole-containing species that exhibit a 10-fold preference for PTP1B relative to that of several dual specificity Cdc25 phosphatases (35).

As noted in the Introduction, we recently found that PTP1B contains two adjacent aryl phosphate binding sites, one at the active site and the other at a proximal noncatalytic site (12). Bisphosphate **1** is bound to PTP1B at these two distinct sites in a mutually exclusive fashion. Each site is approximately 50% occupied (Figure 1). One of the aryl phosphate components of the active site bound **1** engages in interactions that are identical to those found in the corresponding phosphotyrosine-containing structure. This includes a key electrostatic interaction with Arg-221 and an array of hydrogen bond interactions with the amide NH groups of

the Ser-216-Arg-221 backbone. Seventy-seven percent of the nonpolar surface area of active site embedded **1** is buried. The bisphosphate **1** present at the noncatalytic site has one of its aryl phosphate moieties engaged in electrostatic interactions with Arg-24 and Arg-254. Nearly 75% of the nonpolar surface area of **1** bound to the noncatalytic site is enveloped by the enzyme. Two molecules of **1** cannot simultaneously bind to PTP1B due to an otherwise unfavorable steric interaction between the two distal phosphate moieties on each ligand. In contrast, since phosphotyrosine does not contain this double aryl phosphate structural motif, PTP1B is able to simultaneously bind two molecules of phosphotyrosine (12). Since structural features that are important for phosphotyrosine recognition in the catalytic site are conserved among different PTPases, it may be difficult to generate selective inhibitors targeted primarily to the catalytic site. Thus, this newly discovered structural arrangement has potentially important implications in terms of inhibitor design. Can highly selective and potent PTP1B inhibitors be obtained by tethering together two small ligands that can simultaneously occupy both aryl phosphate binding sites? To address this question we have synthesized and tested an array of bis- and tris-difluorophosphonate aromatics.¹ Several of these compounds exhibit PTP1B selectivities of greater than 100-fold.

PTPases not only catalyze the dephosphorylation of phosphotyrosine in active site directed peptides but also utilize nonpeptidic nonnatural aryl phosphates as substrates as well. For example, PTP1 catalyzes the efficient hydrolysis of aryl phosphates **1–3** (11). We decided to employ the basic



structural framework contained within **2** for use in inhibitor design since this species is not only recognized by the active site region of PTP1 but is also readily synthetically available as well. We also note that, except for the missing α -amino moiety, compound **2** is structurally identical to phosphotyrosine itself. The hydrolytically resistant difluorophosphonate analogue (**8**) of **2** was prepared as outlined in Scheme 1.

The effect of the difluorophosphonates on the PTP1B, LAR, PTP α , and VHR-catalyzed pNPP hydrolysis reaction was examined at 25 °C and pH 7.0 (for details, see Materials and Methods). In every case examined, these compounds inhibit the PTPase reaction reversibly and the mode of inhibition is competitive with respect to the substrate (Figure

¹ Although difluorophosphonate was used as a nonhydrolyzable pTyr mimetic in this study, we note that other non-phosphorus-based pTyr surrogates such as *O*-malonyl tyrosine and fluoro-*O*-malonyl tyrosine (37) may also be employed to occupy the pTyr binding sites.

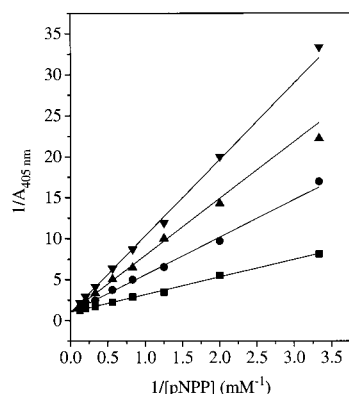
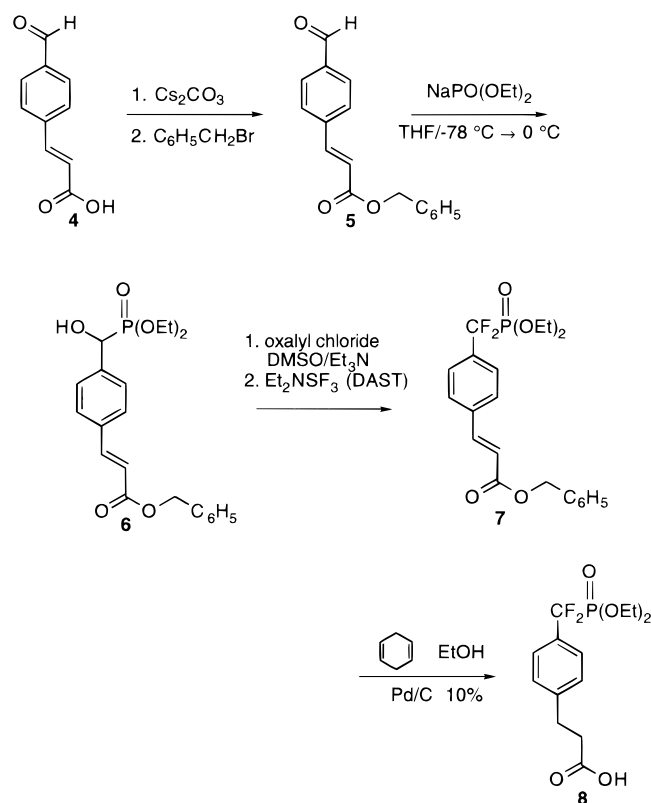


FIGURE 2: Effect of compound **38** on the PTP1B-catalyzed hydrolysis of pNPP. The experiment was performed at 25 °C and pH 7.0. Compound **38** concentrations were 0 μM (■), 1 μM (●), 2 μM (▲), and 3 μM (▼), respectively.

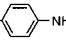
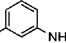
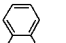
Scheme 1: Synthesis of the Aryl Difluorophosphonate Ligand **8** from 4-Formylcinnamic Acid



2). The catalytic domain of rat PTP1 (residues 1–321) is 97% identical to that of human PTP1B (36). As expected, rat PTP1 and human PTP1B exhibit nearly identical K_i values toward the difluorophosphonates inhibitors prepared in this work (data not shown).

Compound **9** is a modest inhibitor of PTP1B, LAR, and PTP α , and an exceedingly poor inhibitor of the dual specificity PTPase VHR (Table 1). The inhibitory efficacy ($K_i = 420 \pm 32 \mu\text{M}$) of **9** for PTP1B is similar to the K_m ($280 \pm 30 \mu\text{M}$) displayed by the substrate **2** (11). We previously found that the Michaelis constants for several nonnatural aryl phosphate substrates of PTP1 accurately reflects the affinity that these species display for the enzyme (11). This enzyme affinity is recapitulated in the difluorophosphonate derivative **9** as well.

Table 1: K_i Values of Aryl Difluorophosphonates **9**, **10**, **14**–**18** as Competitive Inhibitors (vs *p*-Nitrophenyl Phosphate) of PTP1B, VHR, LAR, and PTP α

Compounds	$^{\circ}\text{O}_3\text{PCF}_2\text{p-C}_6\text{H}_4\text{CH}_2\text{CH}_2\text{CO}-\text{X}$	K_i (μM)			
		PTP1B	VHR	LAR	PTP α
XOH	9	420 ± 30	$18,000 \pm 6,000$	$1,400 \pm 200$	$2,900 \pm 500$
XNH ₂	10	190 ± 10	$27,000 \pm 6,000$	$2,600 \pm 200$	$2,100 \pm 60$
XNH-NHX	14	14 ± 1	$6,000 \pm 30$	230 ± 3	$1,400 \pm 70$
XNH-(CH ₂) ₂ -NHX	15	12 ± 1	$12,000 \pm 2,000$	100 ± 10	470 ± 50
XHN-  -NHX	16	10 ± 1	$4,300 \pm 800$	320 ± 20	$1,300 \pm 200$
XHN-  -NHX	17	5.0 ± 0.1	$21,000 \pm 400$	190 ± 20	$1,000 \pm 200$
XHN-  -NHX	18	12 ± 1	$6,600 \pm 1000$	64 ± 3	$4,500 \pm 900$

Does the free (and presumably negatively charged) carboxylate in **9** augment enzyme affinity? Apparently not, since the corresponding carboxamide-containing species (**10**) exhibits no more than a 2-fold difference in inhibitory potency versus its free acid counterpart for all four PTPases evaluated in this study. This result suggests that **9** can be dimerized or trimerized through an amide linkage without any significant loss in inhibitory activity. We prepared a variety of compounds containing two or more subunits of **9** (Table 1). The dimers were prepared as illustrated in Scheme 2.

Compounds **14** and **15** are better PTPase inhibitors than the parent compounds **9** and **10**. This is especially true with PTP1B, where an order of magnitude improvement in inhibitory efficacy is apparent. In contrast, neither **14** nor **15** are particularly effective inhibitors of VHR or PTP α . Similar trends are observed in the aromatic series **16**–**18**. The meta-substituted derivative **17** is the most effective PTP1B inhibitor in this series. This compound is nearly 2 orders of magnitude more potent as a PTP1B inhibitor compared to that of the parent compound **9**. Furthermore, **17** is 40-fold more selective for PTP1B than for LAR, 200-fold more PTP1B-selective than for PTP α , and 4200-fold more PTP1B-selective than for VHR. We also prepared the benzylic counterparts of **16** and **17**, namely **19** and **20**, respectively (Table 2). Compounds **16** and **19** exhibit nearly identical inhibitory potencies for all four PTPases. The same is true for **17** and **20** as well, with the sole of exception of VHR. Although compound **20** is a weak inhibitor of VHR, it is nevertheless a much better inhibitor for this enzyme than its counterpart **17**. We also prepared the benzoic acid analogue **21**. The latter exhibits inhibitory behavior analogous to that displayed by **17** (with the exception that **21** is a more effective VHR inhibitor than that of **17**). Finally, we synthesized the unsymmetrical bis-difluorophosphonate **22**. Structurally, this compound bears some resemblance to a phosphoTyr–phosphoTyr dyad, with the exception of the missing N- (i.e., amino) and C-termini (i.e., carboxyl) groups. Although the aromatic phosphonates of **22** are more structurally analogous to their naturally occurring phosphotyrosine

Scheme 2: Two-Step Synthesis of Aryl Difluorophosphonate Dimers from the Ligand **8** and Various Diamines

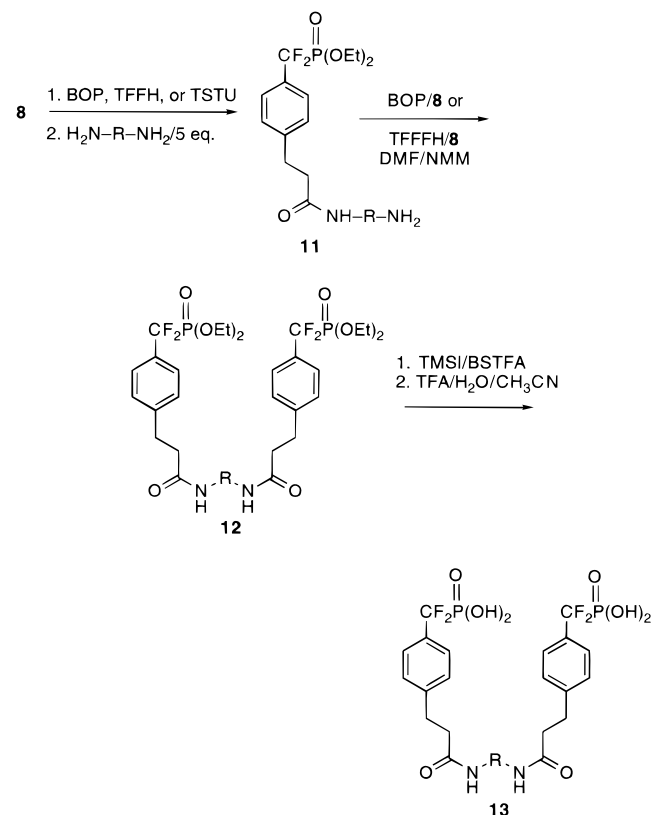
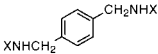
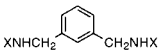
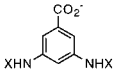
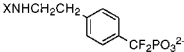
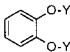
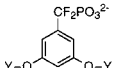


Table 2: K_i Values of Aryl Difluorophosphonates **19**–**24** as Competitive Inhibitors (vs *p*-Nitrophenyl Phosphate) of PTP1B, VHR, LAR, and PTP α

Compounds	K_i (μM)				
	PTP1B	VHR	LAR	PTP α	
$^2\text{O}_3\text{PCF}_2\text{-}p\text{-C}_6\text{H}_4\text{CH}_2\text{CH}_2\text{CO-} = \text{X}$ $^2\text{O}_3\text{PCF}_2\text{-}p\text{-C}_6\text{H}_4\text{CH}_2\text{-} = \text{Y}$					
	19	10 ± 1	$7,100 \pm 3,000$	150 ± 10	$1,200 \pm 100$
	20	11 ± 1	$2,200 \pm 400$	90 ± 5	900 ± 200
	21	3.0 ± 0.1	$2,100 \pm 200$	110 ± 20	7% inhibition at $200 \mu\text{M}$
	22	12 ± 1	$8,000 \pm 3,600$	120 ± 10	no inhibition at $500 \mu\text{M}$
	23	2.7 ± 0.1	$3,900 \pm 600$	50 ± 4	9% inhibition at $250 \mu\text{M}$
	24	3.6 ± 0.2	$3,700 \pm 900$	280 ± 40	$1,700 \pm 200$

counterparts than the phosphonates in **17** and **21**, it is evident that the latter are more formidable PTP1B inhibitors.

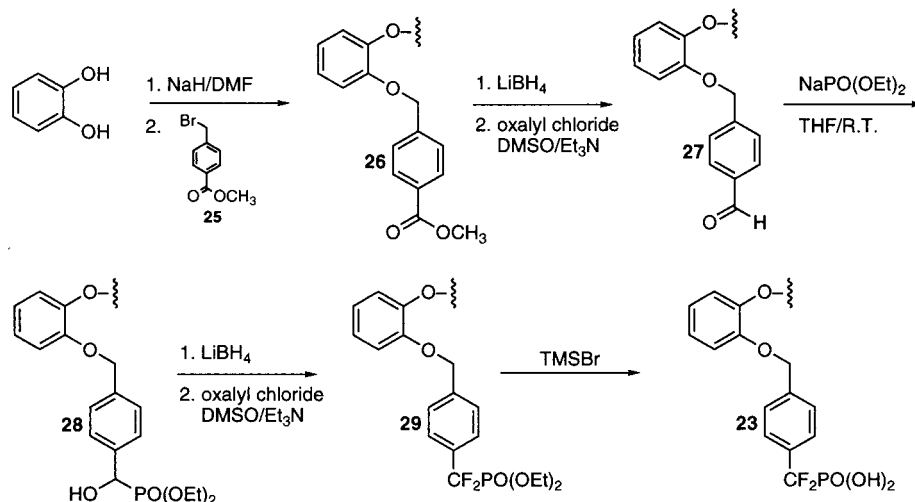
In addition to the amide-linked tethers illustrated in Scheme 2, we also prepared ether-based tethers, **23** and **24** (Scheme 3). Although **23** displays little inhibitory activity

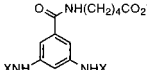
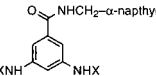
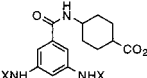
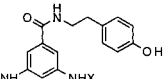
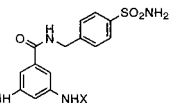
against either VHR or PTP α , it is the most potent LAR inhibitor that we have identified to date. The selectivity that **23** exhibits for PTP1B versus LAR is a relatively modest 18-fold. This PTP1B selectivity improves dramatically with the resorcinol derivative **24** (>75-fold versus LAR). Furthermore, **24**, like its catechol counterpart **23**, is essentially ineffective as an inhibitory agent for VHR or PTP α .

Both **21** and **24** exhibit similar inhibitory profiles against the PTPases examined in this study. In addition, both compounds contain functionality (the carboxylate in **21** and the phosphonate in **24**) upon which additional molecular fragments can be attached. We decided to focus on compound **21** for additional studies due to its more ready synthetic availability and the fact that **24** is susceptible to decomposition over time. Derivatives of **21** [**32**–**38** (Tables 3 and 4)] were prepared as illustrated in Scheme 4. Nearly all of these compounds are highly selective for PTP1B. This includes **34** and **36**, which exhibit a 75- and 370-fold preference for PTP1B versus that of LAR and PTP α , respectively, and **35**, which displays an 81- and 1060-fold selectivity in favor of PTP1B over LAR and PTP α , respectively. However, the highest PTP1B selectivity is exhibited by compounds **37** and **38**. **37** displays a K_i of 2.6 μ M for PTP1B, which is more than 100-fold better than the corresponding values against VHR and LAR (we were unable to detect any inhibition of PTP α at 400 μ M). As an aside, we note that although **37** is a weak inhibitor of VHR, it is nevertheless one of the most potent VHR inhibitory agents identified in this study. In contrast, **38** is not only the most powerful PTP1B-targeted agent that we have identified to date, but it is also an exceedingly poor VHR inhibitor.

The presence of two phosphotyrosine binding sites in PTP1B suggests that inhibitors, which can simultaneously occupy both sites, should exhibit favorable inhibitory properties. Furthermore, based upon a comparison of amino acid sequences and/or known three-dimensional structures, it appears that VHR, LAR, and PTP α all lack the second noncatalytic phosphotyrosine binding site. Consequently, the fact that the difluorophosphonate dimers in this study exhibit a high selectivity for PTP1B versus the three other PTPases is consistent with the notion that these dimers concurrently occupy both phosphotyrosine sites in PTP1B. However, it is also possible that one difluorophosphonate moiety is bound to the active site and the second is merely associated with some positively charged residue on the surface of the enzyme. Indeed, there are a number of such residues (e.g., Lys36, Arg43, Arg45, Arg47, Lys116, and Lys120) within the vicinity of the PTP1B active site. Consequently, we wondered whether three aromatic difluorophosphonates on a single compound might improve inhibitory efficacy even further. Compounds **39** and **40** were synthesized to test this notion. Compound **39** is structurally analogous to **15** with the exception that the former contains an additional ethylamine moiety substituted with an aromatic difluorophosphonate. Interestingly, there is a 6-fold improvement in inhibitory activity versus **15**, with both compounds **39** and **40**. Although these results neither confirm nor refute the

² Preliminary data indicate that exposure of the 3T3L1 adipocyte cell line to compound **33** enhances insulin-mediated uptake of glucose, an observation consistent with PTP1B inhibition (Zhao et al., unpublished results).

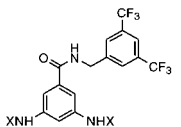
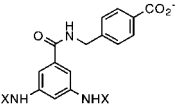
Scheme 3: Synthesis of Catechol-Based Derivatives **23**Table 3: K_i Values of Aryl Difluorophosphonates **32–36** as Competitive Inhibitors (vs *p*-Nitrophenyl Phosphate) of PTP1B, VHR, LAR, and PTP α

Compounds	K_i (μM)			
${}^t\text{O}_3\text{PCF}_2\text{-}p\text{-C}_6\text{H}_4\text{CH}_2\text{CH}_2\text{CO-X}$	PTP1B	VHR	LAR	PTP α
<div></div> 32	1.3 ± 0.1	480 ± 50	76 ± 10	190 ± 70
<div></div> 33	1.0 ± 0.1	220 ± 20	65 ± 19	39 ± 7
<div></div> 34	1.4 ± 0.1	960 ± 80	100 ± 2	540 ± 100
<div></div> 35	1.6 ± 0.1	$3,200 \pm 500$	130 ± 4	$1,700 \pm 500$
<div></div> 36	2.1 ± 0.1	$1,700 \pm 380$	160 ± 30	770 ± 200

possibility that the two phosphotyrosine binding sites in PTP1B are simultaneously occupied by the inhibitors described herein, the inhibitory prowess of **39/40** relative to **15** does suggest that additional interactions between inhibitor and enzyme can be accessed with an appropriately placed third difluorophosphonate moiety.

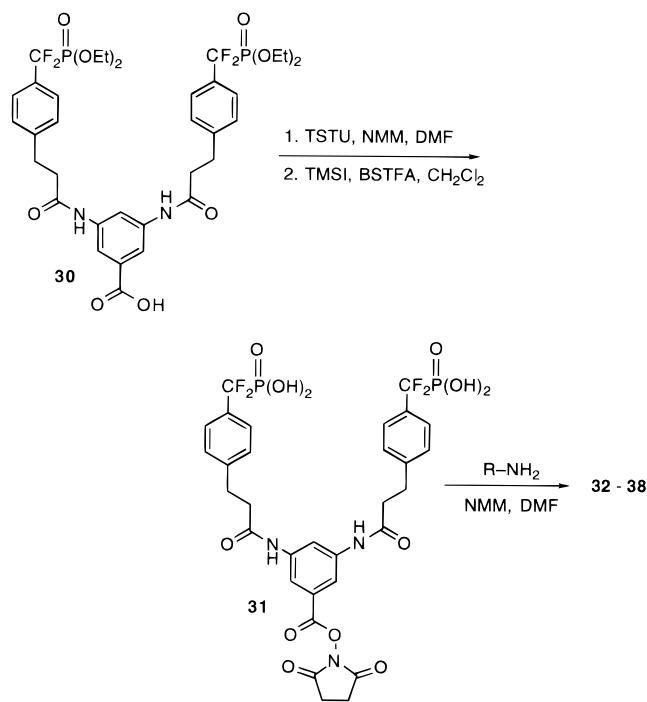
Finally, we assessed the ability of compound **40** to inhibit the PTPase-catalyzed hydrolysis of a pTyr-containing peptide that better mimics the physiological substrates. The substrate we chose was a synthetic tris-phosphotyrosyl dodecapeptide (TRDIpYETDpYpYRK-NH₂) corresponding to the major sites of autophosphorylation in the kinase activation loop of the insulin receptor. We found that compound **40** was a competitive inhibitor of the insulin receptor peptide substrate and displayed a K_i value of $1.73 \pm 0.21 \mu\text{M}$ for PTP1B,

Table 4: K_i Values of Aryl Difluorophosphonates **37–40** as Competitive Inhibitors (vs *p*-Nitrophenyl Phosphate) of PTP1B, VHR, LAR, and PTP α

Compounds	K_i (μM)				
$^t\text{O}_3\text{PCF}_2\text{-p-C}_6\text{H}_4\text{CH}_2\text{CH}_2\text{CO-X}$	PTP1B	VHR	LAR	PTP α	
	37	2.6 ± 0.1	300 ± 100	340 ± 100	no inhibition at 400 μM
	38	0.93 ± 0.03	$3,600 \pm 400$	100 ± 7	120 ± 30
$\text{XN}(\text{CH}_2\text{CH}_2\text{NHX})_2$	39	1.8 ± 0.1	$4,300 \pm 1,300$	60 ± 3	530 ± 70
$\text{N}(\text{CH}_2\text{CH}_2\text{NHX})_3$	40	1.4 ± 0.1	$3,100 \pm 600$	60 ± 3	$1,300 \pm 120$

$61.8 \pm 7.4 \mu\text{M}$ for LAR, and $1150 \pm 170 \mu\text{M}$ for PTP α . These results are similar to those obtained with *p*NPP as a substrate (Table 4). Because the inhibitors described in this report were PTPase active site directed, it was expected that identical K_i values be obtained irrespective of the substrates used.

In summary, we have previously shown that PTP1B contains two proximal aryl phosphate binding sites. Compounds such as **1** exhibit an equivalent affinity for both sites. As a consequence, we prepared an array of bis- and tris-(aryl difluorophosphonates) that are designed to simultaneously occupy both sites. The free energy of binding from the occupancy of these sites should result in enhanced enzyme affinity. Indeed, the bis-aryl derivative **38** is a 450-fold more potent PTP1B inhibitor than its mono-aryl counterpart **9**. Furthermore, the interaction of an inhibitor with two independent sites should result in high selectivity if one of these sites is not present in other PTPases. To the best of our knowledge, the most selective PTP1B inhibitors identified to date exhibit a 10-fold preference relative to the dual specificity *cdc25* phosphatases (35). The inhibitors described herein likewise display a preference for PTP1B versus a dual specificity phosphatase (i.e. VHR), but one that is 3–4 orders of magnitude in size. This high selectivity

Scheme 4: Synthesis of 3,5-Diaminobenzoic Acid-Based Dimers **32**–**38**

is presumably a consequence of the known dissimilarities in primary and tertiary structures between the tyrosine-specific PTPases (**38**–**39**) and the dual specificity phosphatases (**40**–**41**). Remarkably, compounds such as **37** and **38** not only display a strong PTP1B selectivity compared to a dual specificity phosphatase but also exhibit a >100-fold preference for PTP1B relative to the other tyrosine-specific PTPases implicated in the insulin-driven signaling pathway. These results demonstrate that it should be feasible to develop potent and PTPase-selective inhibitors for individual members of the large phosphatase family of enzymes. Potent, yet highly selective, PTPase inhibitors should not only prove useful in dissecting the precise roles played by specific PTPases in the insulin-mediated signal transduction pathway,² but may ultimately furnish a molecular basis upon which therapeutically useful agents can be designed.

REFERENCES

- Lawrence, D. S., and Niu, J. (1998) *Pharmacol. Ther.* **77**, 81–114.
- Zhang, Z.-Y. (1998) *CRC Crit. Rev. Biochem. Mol. Biol.* **33**, 1–52.
- Tonks, N. K., Diltz, C. D., and Fischer, E. H. (1988) *J. Biol. Chem.* **263**, 6722–30.
- Tonks, N. K., Diltz, C. D., and Fischer, E. H. (1988) *J. Biol. Chem.* **263**, 6731–7.
- Goldstein, B. J. (1993) *Receptor* **3**, 1–15.
- Ahmad, F., Li, P. M., Meyerovitch, J., and Goldstein, B. J. (1995) *J. Biol. Chem.* **270**, 20503–8.
- Kenner, K. A., Anyanwu, E., Olefsky, J. M., and Kusari, J. (1996) *J. Biol. Chem.* **271**, 19810–6.
- Wiener, J. R., and Kerns, B. J., Harvey, E. L., Conaway, M. R., Iglehart, J. D., Berchuck A., and Bast, R. C., Jr. (1994) *J. Natl. Cancer Inst.* **86**, 372–8.
- Liu, F., Hill, D. E., and Chernoff, J. (1996) *J. Biol. Chem.* **271**, 31290–95.
- Liu, F., and Chernoff, J. (1997) *Biochem. J.* **327**, 139–45.
- Chen, L., Montserat, J., Lawrence, D. S., and Zhang, Z. Y. (1996) *Biochemistry* **35**, 9349–54.
- Puius, Y. A., Zhao, Y., Sullivan, M., Lawrence, D. S., Almo S. C., and Zhang, Z. Y. (1997) *Proc. Natl. Acad. Sci. U S A.* **94**, 13420–5.
- Middleton, W. (1975) *J. Org. Chem.* **40**, 574–8.
- Hengge, A. C., Sowa, G., Wu, L., and Zhang, Z.-Y. (1995) *Biochemistry* **34**, 13982–13987.
- Guan, K. L., and Dixon, J. E. (1991) *Anal. Biochem.* **192**, 262–267.
- Pot, D. A., Woodford, T. A., Remboutsika, E., Haun, R. S. and Dixon, J. E. (1991) *J. Biol. Chem.* **266**, 19688–19696.
- Zhang, Z.-Y., Wu, L., and Chen, L. (1995) *Biochemistry* **34**, 16088–16096.
- Zhang, Z.-Y., and Van Etten, R. L. (1991) *J. Biol. Chem.* **266**, 1516–1525.
- Zhang, Z.-Y., Thieme-Sefler, A. M., Maclean, D., Roeske, R., and Dixon, J. E. (1993) *Anal. Biochem.* **211**, 7–15.
- Ishibashi, T., Bottara, D. P., Chan, A., Miki, T., and Aaronson, S. A. (1992) *Proc. Natl. Acad. Sci. U.S.A.* **89**, 12170–12174.
- Guan, K. L., Broyles, S., and Dixon, J. E. (1991) *Nature* **350**, 359–361.
- Zhang, W. R., Li, P. M., Oswald, M. A., and Goldstein, B. J. (1996) *Mol. Endocrinol.* **10**, 575–84.
- Mooney, R. A., Kulas, D. T., Bleyle, L. A., and Novak, J. S. (1997) *Biochem. Biophys. Res. Commun.* **235**, 709–12.
- Ahmad, F., and Goldstein, B. J. (1997) *J. Biol. Chem.* **272**, 448–57.
- Lammers, R., Moller, N. P., and Ullrich, A. (1997) *FEBS Lett.* **404**, 37–40.
- Seely, B. L., Staubs, P. A., Reichart, D. R., Berhanu, P., Milarski, K. L., Saltiel, A. R., Kusari, J., and Olefsky, J. M. (1996) *Diabetes* **45**, 1379–85.
- Ahmad, F., Azevedo, J. L., Cortright, R., Dohm, G. L., and Goldstein, B. J. (1997) *J. Clin. Invest.* **100**, 449–58.
- Li, P. M., Zhang, W. R., and Goldstein, B. J. (1996) *Cell Signal.* **8**, 467–73.
- Burke, T. R. Jr., Kole, H. K., and Roller, P. P. (1994) *Biochem. Biophys. Res. Commun.* **204**, 129–34.
- Chen, L., Wu, L., Otaka, A., Smyth, M. S., Roller, P. P., Burke, T. R., Jr., den Hertog, J., and Zhang, Z. Y. (1994) *Biochem. Biophys. Res. Commun.* **216**, 976–84.
- Kole, H. K., Smyth, M. S., Russ, P. L., and Burke, T. R. Jr. (1995) *Biochem. J.* **311** (Pt 3), 1025–31.
- Burke, T. R. Jr. Ye, B., Yan, X., Wang, S., Jia, Z., Chen, L., Zhang, Z. Y., and Barford, D. (1996) *Biochemistry* **35**, 15989–96.
- Moran, E. J., Sarshar, S., Cargill, J. F., Shahbaz, M. M., Lio, A., Mjalli, A. M. M., and Armstrong, R. W. (1995) *J. Am. Chem. Soc.* **117**, 10787–10788.
- Taylor, W. P., Zhang, Z. Y., and Widlanski, T. S. (1996) *Bioorg. Med. Chem.* **4**, 1515–20.
- Rice, R. L., Rusnak, J. M., Yokokawa, F., Yokokawa, S., Messner, D. J., Boynton, A. L., Wipf, P., and Lazo, J. S. (1997) *Biochemistry* **36**, 15965–74.
- Zhang, Z.-Y. (1995) *J. Biol. Chem.* **270**, 11199–11204.
- Roller, P. P., Wu, L., Zhang, Z.-Y., and Burke, T. R. (1998) *Bioorg. Med. Chem. Lett.* **8**, 2149–2150.
- Barford, D., Flint, A. J., and Tonks, N. K. (1994) *Science* **263**, 1397–1404.
- Bilwes, A. M. den Hertog, J., Hunter, T., and Noel, J. P. (1996) *Nature* **382**, 555–559.
- Yuvaniyama, J., Denu, J. M., Dixon, J. E., and Saper, M. A. (1996) *Science* **272**, 1328–1331.
- Fauman, E. B., Cogswell, J. P., Lovejoy, B., Rocque, W. J., Holmes, W., Montana, V. G., Piwnicka-Worms, H., Rink, M. J., and Saper, M. A. (1998) *Cell* **93**, 617–625.